Eur Biophys J (2004) 33: 651–655
DOI 10.1007/s00249-004-0390-7

BIOPHYSICS LETTER

Ewgeni B. Starikow · Lennart Nilsson
Martin Hülsmeyer

A single residue exchange between two HLA-B27 alleles triggers increased peptide flexibility

Received: 9 January 2004 / Accepted: 15 January 2004 / Published online: 10 March 2004

Abstract For more than 30 years, human leukocyte antigen B27 (HLA-B27) has been known to be closely related to the autoimmune disease ankylosing spondylitis, yet little is known about the molecular mechanisms of pathogenesis. Crystal structures of two closely related, but differently disease-associated, subtypes (B*2705 and B*2709) also did not resolve this situation as they revealed the bound nonapeptide in essentially identical conformations. As the peptide is part of putative binding epitopes for the T cell receptor, we performed molecular dynamics simulations to gain deeper insight into the dynamic behaviour of HLA-B27 molecules. We find increased flexibility of the peptide in the binding groove of subtype B*2709 due to weaker interactions in the F pocket. Possible implications of this flexibility for T cell recognition and signalling are discussed.

Keywords Human leukocyte antigen · Major histocompatibility complex · Molecular dynamics · Spondyloarthropathies · Surface flexibility

Abbreviations β_2m: β_2-microglobulin · AS: ankylosing spondylitis · CDR: complementarity determining region · HC: heavy chain · HLA: human leukocyte antigen · MD: molecular dynamics · MHC: major histocompatibility complex · pMHC: peptide-loaded MHC · RMSD: root mean square deviation · RMSF: root mean square fluctuation · TCR: T cell receptor

E. B. Starikow · L. Nilsson (✉)
Department of Biosciences at NOVUM, Karolinska Institutet,
141 57 Huddinge, Sweden
E-mail: lennart.nilsson@biosci.ki.se

M. Hülsmeyer
Institute for Crystallography, Free University Berlin,
14195 Berlin, Germany

Introduction

Major histocompatibility complex (MHC) class I molecules have key functions in the immune system's surveillance for foreign pathogens (Klein et al. 1993). They are heterotrimeric protein complexes (Fig. 1A), consisting of a membrane-anchored heavy chain (HC), noncovalently linked to β_2-microglobulin (β_2m) and a peptide, usually 8–10 residues long. This peptide is generated proteolytically from intracellular proteins (Saper et al. 1991) and accommodated in a binding groove of the heavy chain that features six pockets termed A to F (Madden 1995). At the cell surface, the peptide is presented to T cell receptors (TCRs) residing on cytotoxic T cells. If the TCR recognizes the peptide to be non-self, the presenting cell is targeted for death (Townsend and Bodmer 1989).

Crystal structures of peptide-loaded MHC (pMHC) complexed with a TCR have revealed a roughly diagonal binding mode of the TCR on top of the pMHC (see Rudolph and Wilson 2002 for review). The footprint (or TCR epitope) on the pMHC usually comprises both helices to a variable extent and the accessible section of the peptide, which commonly bulges out from the binding groove (Fig. 1). Six receptor loops [similar to antibody hypervariable complementarity determining region (CDR) loops] are used for this interaction: CDR1 and CDR2 loops usually contact the human leukocyte antigen (HLA) helices, while the CDR3 loops interact with the peptide. Crystallographic studies have shown that the latter loops undergo large conformational changes upon binding (Reiser et al. 2002).

The human MHC molecule HLA-B27 is strongly associated with ankylosing spondylitis (AS), which belongs to a group of inflammatory autoimmune disorders (Ramos and Lopez de Castro 2002). Although the molecule itself appears as the strongest predisposing factor for AS pathogenesis (Brewerton et al. 1973; Schlosstein et al. 1973), little is known about the underlying molecular mechanism(s). Recently, the subtypes

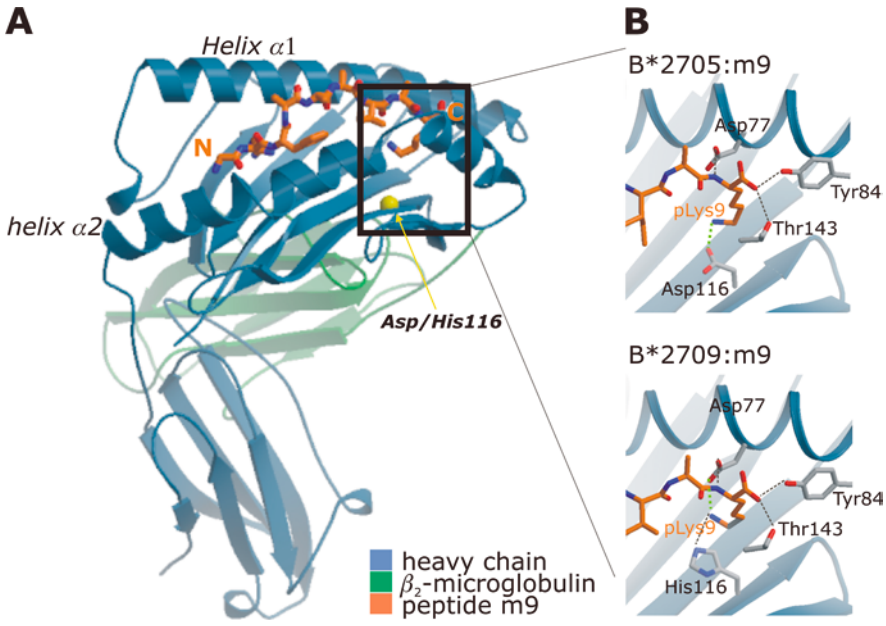

Fig. 1 **A** Ribbon representation of HLA-B*2709:m9, with the heavy chain (HC) depicted in *blue* and β_2-microglobulin in *green*. The m9 peptide is shown as *stick model* in the binding groove of the HC, which is formed by an eight-stranded β-sheet and two long helices, α1 and α2. The location of the B*2705/09 subtype-specific difference in residue 116 is indicated in *yellow*. **B** The binding situation of the C-terminal peptide residue pLys9 of each subtype together with residue 116 and further residues shaping the F pocket. Hydrogen bonds are shown as *black*, salt bridges as *green dotted lines*; HC and peptide are color-coded as in **A**

HLA-B*2705 and B*2709 were employed in a comparative crystallographic study (Hülsmeyer et al. 2002). In both structures the same model peptide "m9" (GRFAAAIAK) is present in the binding groove. The amino acid sequences of the two HLA molecules differ in only one residue of the heavy chain (His116 in B*2709 versus Asp116 in B*2705), though subtype B*2705 shows strong disease association while B*2709 does not (Khan 2002). Residue 116 is part of the F pocket which accommodates the peptide C-terminus and consequently is inaccessible for a TCR (Fig. 1) which binds on the composite surface of the pMHC. The main finding of the report (Hülsmeyer et al. 2002) is that m9 is bound in essentially the same conformation in either subtype, thus generating highly similar topologic and electrostatic molecular surfaces. The question arises of how a TCR can distinguish the HLA molecules and generate a distinct signal when shape and charge are excluded for discrimination. We have addressed this issue by performing molecular dynamics simulations to describe the dynamic characteristics of these HLA molecules, i.e. properties which are not accessible when using only crystallographic data. Assessing the role of the protein dynamics is of crucial immunological importance, since surface motions and flexibility of the HLA binding domain together with the complexed peptide (these two constitute putative TCR epitopes) should directly influence T cell binding and signalling.

Methods

Molecular dynamics (MD) simulations were performed with the CHARMM program (Brooks et al. 1983) using the all-atom force field version 22 (MacKerell et al. 1998). The atomic coordinates for the HLA-B*2705 and HLA-B*2709 calculations were taken from the Protein Databank (Berman et al. 2002) (PDB ID 1jge and 1k5n; Hülsmeyer et al. 2002). Each of the two systems consists of three chains: the heavy chain (276 residues), β_2-microglobulin (100 residues), and the nonapeptide m9, which is non-covalently connected to the HC. The primary structures of B*2705 and B*2709 differ only at position 116 of the HC; it is a negatively charged aspartate in B*2705, but in B*2709 it is a histidine. In both structures, residue 116 is in direct contact with the m9 peptide (Hülsmeyer et al. 2002; Fig. 1B). However, the physicochemical nature of this contact is obviously different for the two systems.

Each of the two systems was placed into a water shell of 7 Å thickness (Sen and Nilsson 1999) using the TIP3 (Jorgensen et al. 1983) water model. This amounted to 8184 water molecules around B*2705 and 8870 water molecules around B*2709, with 13 Na^+ (12 Na^+) cations added to B*2705 (B*2709), to ensure electroneutrality. All covalent bonds to hydrogen atoms were constrained using the SHAKE algorithm (Ryckaert et al. 1977), allowing a 2 fs time step in the MD simulations. Electrostatic and van der Waals energies and forces were smoothly shifted to zero at a 12 Å cut-off, which has been shown to work well with biopolymer polyanions (Norberg and Nilsson 2000). The neighbour list was generated to 14 Å and updated whenever any atom had moved >1 Å since the last update. The systems were first minimized for 200 steps with steepest descent and adopted basis-set Newton–Raphson methods, followed by 60 ps heating and equilibration. After this a 3 ns trajectory was generated at 300 K for the analysis. The water evaporation from the water drop surfaces was negligible during the simulations (less than 500 water molecules in each case).

Root mean square deviations (RMSD) from the X-ray structures along the MD trajectories, as well as root mean square fluctuations (RMSF) around the structures averaged along the MD trajectories, were computed after removal of overall rotation and translation of the solutes. To remove the above motions, we selected β_2 m to be the reference subunit for the superimpositions, since it is situated far away from residue 116 where the mutation under study is located. Moreover, RMSFs were converted to temperature factors [$B = 8\pi^2(\mathrm{RMSF})^2/3$] and further averaged over each residue.

Statistics of hydrogen bonding between the m9 peptide and the heavy chain were analyzed as well, with a hydrogen bond defined as being present when the acceptor and hydrogen atoms are closer than 2.4 Å.

Results

From the time evolution of the overall RMSD for all heavy atoms (Fig. 2) the trajectories were judged to be

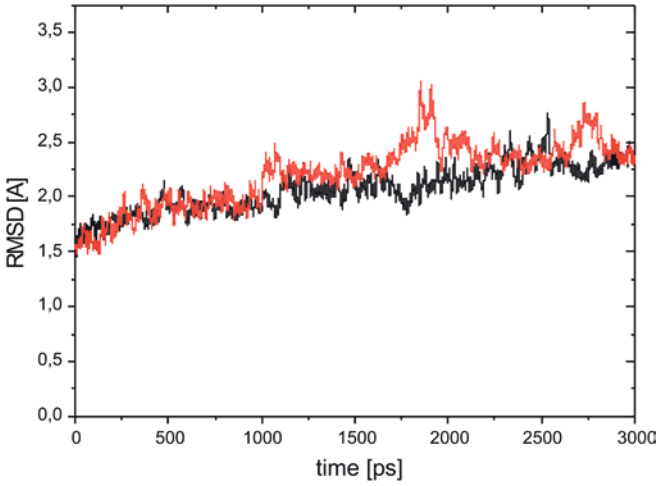

Fig. 2 Time plots of the overall root-mean-square deviations (RMSDs) from the crystal structures for B*2705:m9 (*black*) and B*2709:m9 (*red*)

stable and well equilibrated after 0.3 ns; the remaining 2.7 ns were used in all analyses presented below.

A comparison of the residue-averaged RMSDs computed for all atoms between the calculated average structures and the corresponding crystal structures for B*2705:m9 and B*2709:m9 (Fig. 3A) shows differences between the crystal and simulated structures only at individual positions, thus indicating a stable simulation. The *B*-factors computed from the RMSFs (Fig. 3B) are qualitatively similar to the crystallographic *B*-factors (Hülsmeyer et al 2002), being low in the tightly packed protein core and high in flexible exposed loop regions. No significant differences are detectable in the protein RMSFs between the subtypes. However, the flexibility of the peptide is apparently dependent on the binding groove context: m9 is more mobile in B*2709 than in B*2705, especially in its C-terminal half (see inset of Fig. 3B). The differences in peptide flexibility seem to be related to the architecture of the subtype-specific F pocket. Specific distance and angle transitions in this region in B*2709:m9 indicate a looser coordination and consequently higher mobility of m9 in this subtype (Figs. 4 and 5).

Analysis of hydrogen bonding statistics between the m9 peptide and heavy chain along the MD trajectory reveals that the contact between Asp116-OD2 and pLys9-NZ in B*2705 is a robust salt bridge (occupancy 94%), but the interaction between His116-NE2 and pLys9-NZ in B*2709 is very weak (occupancy 6%; Fig. 4A). In the Asp77-OD1–pLys9-N distance plot (Fig. 4B) for B*2709 a transition is visible after 2.2 ns of the MD simulation. Together with a significant widening of the binding groove (in the range of 1.5–2 Å between the helices) this evolution leads to a full destruction of this (though anyway weak) contact. In B*2705 the occupancy of this Asp77-OD1–Lys9-N contact is 99% but only 51% in B*2709, demonstrating a weaker fixation of the peptide to the binding groove in the latter

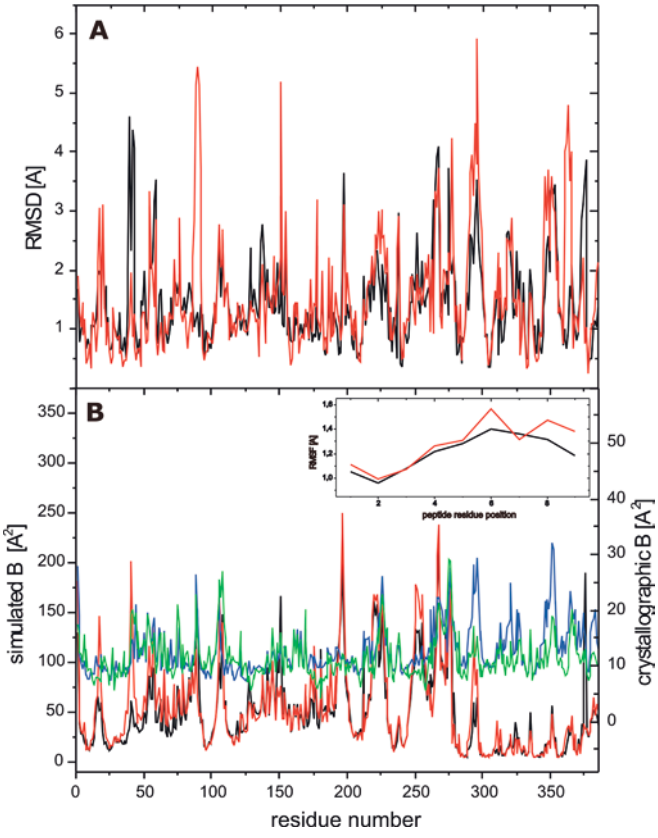

Fig. 3 **A** Comparison between the RMSDs per residue for B*2705:m9 (*black*) and B*2709:m9 (*red*). **B** Comparison between the root-mean-square fluctuations (RMSFs) converted to *B*-factors per residue for B*2705:m9 (*black*) and B*2709:m9 (*red*). Crystallographic *B*-factors are shown in *blue* (B*2705:m9) and *green* (B*2709:m9). Residue numbers 1–276 represent the HC, 277–377 are β_2-microglobulin and the last nine residues are the m9 peptide. *Inset*: RMSF per residue plot for the m9 peptide only

subtype. In contrast, Asp77-OD2 is contacted throughout the trajectory with pLys9-NZ in B*2709, but this contact is missing in B*2705:m9 (Fig. 4C), in full agreement with the crystal structures.

Two further contacts with the peptide C-terminus show a subtype-specific pattern: first, the durable contact between Thr143 and pLys9-OT2 in B*2705 (occupancy 99%; Fig. 4D) is completely absent in B*2709; and second, Tyr84-OH is involved in a rather strong H-bond with pLys9-OT2 in B*2709 after 1.6 ns (occupancy 84%), but in B*2705 no such interaction is present (Fig. 4E). Additional flexibility in the F pocket is generated by the instability of the important Asp74OD1–Lys70-NZ salt bridge in B*2709 (occupancy 18%, B*2705 occupancy 92%; Fig. 4F). Like in Fig. 4B, a transition is visible at 2.2 ns, suggesting a correlation between these incidents.

Taken together, these data indicate that the m9 peptide is less tightly bound in the B*2709 binding groove than it is in B*2705. During the simulation, large fluctuations are visible (Fig. 4) and after 3 ns the peptide has significantly moved out of the B*2709 groove (> 2 Å; Fig. 5), which makes the different contacts to

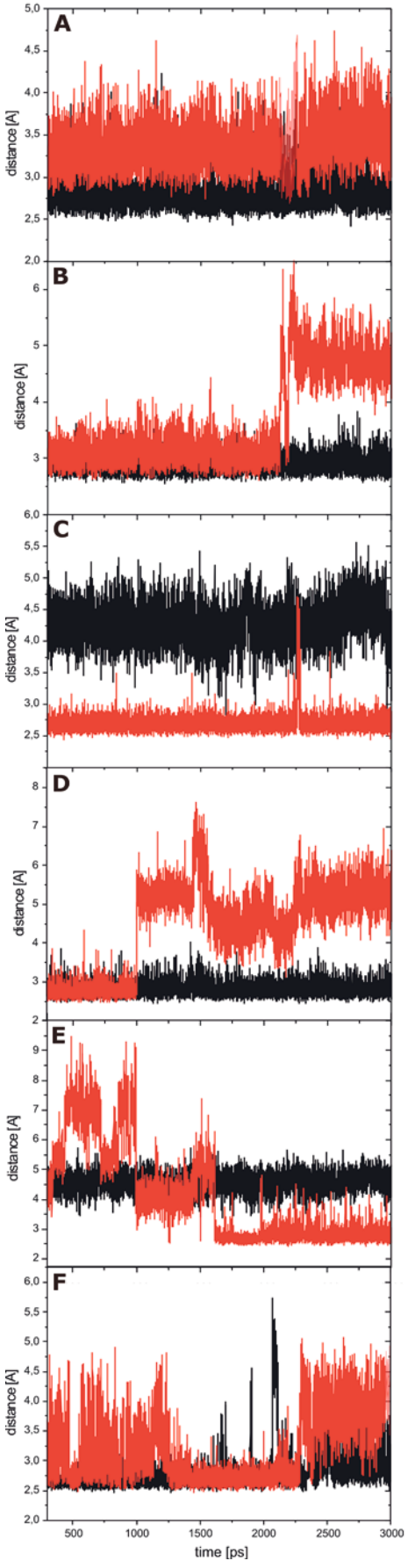

◀

Fig. 4A–F Time series for distances between residues in the F pocket; values for B*2705:m9 are shown in *black*, values for B*2709:m9 in *red*. **A** pLys9^{NZ}–Asp116^{OD2}(B*2705), pLys9^{NZ}–His116^{ND2}(B*2709); **B** pLys9^{N}–Asp77^{OD1}; **C** pLys9^{NZ}–Asp77^{OD2}; **D** pLys9^{OT2}–Thr143^{OG1}; **E** pLys9^{OT2}–Tyr84^{OH}; **F** Asp74^{OD1}–Lys70^{NZ}

Tyr84 and Thr143 understandable. In the case of B*2705, only minor flexibility is observable.

Discussion

Our MD simulations show significant differences in the mobility of model peptide m9 loaded to HLA-B*2705 and B*2709. The interplay between bound peptide, specifically the C-terminal pLys9 residue, the subtype-specific residue 116 and additional F pocket residues seems to be crucial for this result. In the case of B*2705:m9, pLys9 can be accommodated well in the F pocket and strong bonds attach it firmly to the base of the binding groove (in particular the salt bridge pLys9–Asp116), resulting in limited freedom to move. In contrast, tight binding of the pLys9 is hampered in B*2709 due to the presence of His116. The steric requirements and chemical nature of the histidine side chain allow the formation of only one (long) H-bond to pLys9 and leads to a weaker anchoring to the binding groove floor. Instead, pLys9 binds to Asp77 (helix α1), which, in turn, seems to increase the mobility of both the peptide and at least some side chains of the B*2709 binding groove (e.g. Tyr84). Superimpositions (Fig. 5) reveal that m9 clearly demonstrates more flexibility in B*2709 than in B*2705 and a motional trend out of the groove. Asp77 and His116 therefore appear to play an important function as ''switching'' residues which could possibly be the physicochemical key for triggering enhanced peptide mobility. To verify this hypothesis, a MD simulation with a pGlu9 in the F pocket of B*2709 should considerably decrease the flexibility, as Glu can be supposed to interact more favourably with His116.

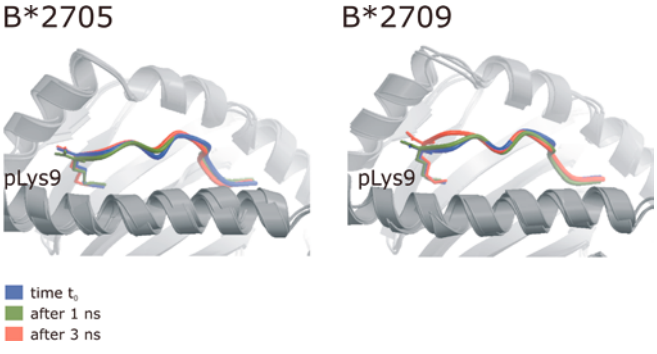

Fig. 5 Superimpositions of the binding groove at different time-points. The groove is depicted in *grey*, the Cα trace and pLys9 are color-coded according to the length of the trajectory (see legend). The large positional shift of the peptide in the binding groove of B*2709 is clearly visible

Wu et al. (2002) have shown that the association of the TCR with a peptide-loaded MHC (pMHC) is a two-step process consisting of docking the TCR to the pMHC in a largely peptide-independent fashion, followed by stabilization of the pMHC:TCR complex driven by formation of peptide–TCR contacts. The flexibility observed in the TCR antigen binding site (CDR loops) thereby acts as an important feature for optimizing the fit of the initial complex (Boniface et al. 1999; Reiser et al. 2002). Experiments by Willcox et al. (1999) similarly suggested that the TCR and/or pMHC possess flexibility in their interaction surfaces that is stabilized upon binding. We think that the peptide mobility we have detected in our MD simulations represents exactly this feature. Moreover, the extra "entropic" contribution to the molecular recognition could represent a discrimination possibility of otherwise structurally identical HLA complexes.

The pMHC:TCR interaction has been described as a low-affinity interaction (Davis et al. 1998; Willcox et al. 1999), making it susceptible to disturbances. The findings of Wu et al. (2002) suggest that it is likely that mobility in the peptide affects the binding of the TCR to the pMHC. This can be favourable or not: flexibility may impair binding, thus providing a means to discriminate structurally similar pMHCs with a kind of "motional control". On the other hand, flexibility may also give rise to cross reactivity, as the interaction surfaces are only ambiguously defined. This could also be the case in differentially disease-associated HLA-B27 molecules, where we detected subtype-specific peptide mobility.

Unfortunately, the model nature of the m9 peptide complicates the evaluation of the physiological relevance of our results. As biological data and TCRs are not available for non-natural peptides, we cannot verify how or to which extent binding and/or T cell signalling is influenced. However, increased flexibility and modified TCR–pMHC recognition may represent an effective means for a TCR to discriminate structurally similar pMHCs. To validate our hypothesis, MD simulations are underway with further pMHC molecules for which more biological data are available than is the case for HLA-B27.

References

Berman HM, Battistuz T, Bhat TN, Bluhm WF, Bourne PE, Burkhardt K, Feng Z, Gilliland GL, Iype L, Jain S, Fagan P, Marvin J, Padilla D, Ravichandran V, Schneider B, Thanki N, Weissig H, Westbrook JD, Zardecki C (2002) The Protein Data Bank. Acta Crystallogr Sect D 58:899–907

Boniface JJ, Reich Z, Lyons DS, Davis MM (1999) Thermodynamics of T cell receptor binding to peptide-MHC: evidence for a general mechanism of molecular scanning. Proc Natl Acad Sci USA 96:11446–11451

Brewerton DA, Hart FD, Nicholls A, Caffrey M, James DC, Sturrock RD (1973) Ankylosing spondylitis and HLA-B27. Lancet 1:904–907

Brooks BR, Bruccoleri RE, Olafson BD, States DJ, Swaminathan S, Karplus M (1983) CHARMM: a program for macromolecular energy minimization and dynamics calculations. J Comput Chem 4:187–217

Davis MM, Boniface JJ, Reich Z, Lyons D, Hampl J, Arden B, Chien Y (1998) Ligand recognition by alpha beta T cell receptors. Annu Rev Immunol 16:523–44

Hülsmeyer M, Hillig RC, Volz A, Ruhl M, Schröder W, Saenger W, Ziegler A, Uchanska-Ziegler B (2002) HLA-B27 subtypes differentially associated with disease exhibit subtle structural alterations. J Biol Chem 277:47844–47853

Jorgensen WL, Chandrasekhar J, Madura J, Impey RW, Klein ML (1983) Comparison of simple potential functions for simulating liquid water. J Chem Phys 79:926–935

Khan MA (2002) Update on spondyloarthropathies. Ann Intern Med 136:896–907

Klein J, Satta Y, O'Huigin C, Takahata N (1993) The molecular descent of the major histocompatibility complex. Annu Rev Immunol 11:269–95

MacKerell AD Jr, Bashford D, Belott M, Dunbrack RL, Evenseck JD, Field MJ, Fischer S, Gao J, Gua H, Ha S, Joseph-McCarthy D, Kuchnir L, Kuczera K, Lau FTK, Mattos C, Michnik S, Ngo T, Nguyen DT, Prodhom B, Reiher WE, Roux B, Schlenkrich M, Smith JC, Stote R, Straub J, Wiórkiewicz-Kuczera J, Yin D, Karplus M (1998) All-atom empirical potential for molecular modeling and dynamics studies of proteins. J Phys Chem B 102:3586–3616

Madden DR (1995) The three-dimensional structure of peptide-MHC complexes. Annu Rev Immunol 13:587–622

Norberg J, Nilsson L (2000) On the truncation of long-range electrostatic interactions in DNA. Biophys J 79:1537–1553

Ramos M, Lopez de Castro JA (2002) HLA-B27 and the pathogenesis of spondyloarthritis. Tissue Antigens 60:191–205

Reiser JB, Gregoire C, Darnault C, Mosser T, Guimezanes A, Schmitt-Verhulst AM, Fontecilla-Camps JC, Mazza G, Malissen B, Housset D (2002) A T cell receptor CDR3beta loop undergoes conformational changes of unprecedented magnitude upon binding to a peptide/MHC class I complex. Immunity 16:345–354

Rudolph MG, Wilson IA (2002) The specificity of TCR/pMHC interaction. Curr Opin Immunol 14:52–65

Ryckaert JP, Ciccotti G, Berendsen HJC (1977) Numerical Integration of the cartesian equations of motion of a system with constraints: molecular dynamics of n-alkanes. J Comput Phys 23:327–341

Saper MA, Bjorkman PJ, Wiley DC (1991) Refined structure of the human histocompatibility antigen HLA-A2 at 2.6 Å resolution. J Mol Biol 219:277–319

Schlosstein L, Terasaki PI, Bluestone R, Pearson CM (1973) High association of an HL-A antigen, B27, with ankylosing spondylitis. N Engl J Med 288:704–706

Sen S, Nilsson L (1999) Structure, interaction, dynamics and solvent effects on the DNA-EcoRI complex in aqueous solution from molecular dynamics simulation. Biophys J 77:1782–1800

Townsend A, Bodmer H (1989) Antigen recognition by class I-restricted T lymphocytes. Annu Rev Immunol 7:601–24

Willcox BE, Gao GF, Wyer JR, Ladbury JE, Bell JI, Jakobsen BK, van der Merwe PA (1999) TCR binding to peptide-MHC stabilizes a flexible recognition interface. Immunity 10:357–365

Wu LC, Tuot DS, Lyons DS, Garcia KC, Davis MM (2002) Two-step binding mechanism for T-cell receptor recognition of peptide MHC. Nature 418:552–556